

# Rotational Spectrum and Conformational Composition of Cyanoacetaldehyde, a Compound of Potential Prebiotic and Astrochemical Interest

Harald Møllendal,<sup>\*,†</sup> Laurent Margulès,<sup>‡</sup> Roman A. Motiyenko,<sup>‡</sup> Niels Wessel Larsen,<sup>§</sup> and Jean-Claude Guillemin<sup>||</sup>

<sup>†</sup>Centre for Theoretical and Computational Chemistry (CTCC), Department of Chemistry, University of Oslo, P.O. Box 1033 Blindern, NO 0315 Oslo, Norway

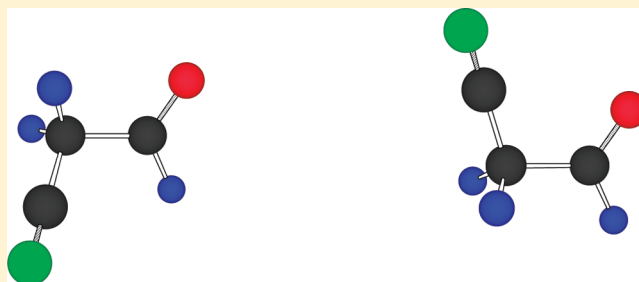
<sup>‡</sup>Laboratoire de Physique des Lasers, Atomes, et Molécules, UMR CNRS 8523, Université de Lille I, F-59655 Villeneuve d'Ascq Cédex, France

<sup>§</sup>Department of Chemistry, University of Copenhagen, The H. C. Ørsted Institute, Universitetsparken 5, DK 2100 Copenhagen Ø, Denmark

<sup>||</sup>Sciences Chimiques de Rennes, École Nationale Supérieure de Chimie de Rennes, CNRS, UMR 6226, Avenue du Général Leclerc, CS 50837, 35708 Rennes Cedex 7, France

## Supporting Information

**ABSTRACT:** The rotational spectrum of cyanoacetaldehyde ( $\text{NCCH}_2\text{CHO}$ ) has been investigated in the 19.5–80.5 and 150–500 GHz spectral regions. It is found that cyanoacetaldehyde is strongly preferred over its tautomer cyanovinylalcohol ( $\text{NCCH}=\text{CHOH}$ ) in the gas phase. The spectra of two rotameric forms of cyanoacetaldehyde produced by rotation about the central C–C bond have been assigned. The C–C–C–O dihedral angle has an unusual value of  $151(3)^\circ$  from the synperiplanar ( $0^\circ$ ) position in one of the conformers denoted **I**, while this dihedral angle is exactly synperiplanar in the second rotamer called **II**, which therefore has  $C_s$  symmetry. Conformer **I** is found to be preferred over **II** by  $2.9(8)$  kJ/mol from relative intensity measurements. A double minimum potential for rotation about the central C–C bond with a small barrier maximum at the exact antiperiplanar ( $180^\circ$ ) position leads to Coriolis perturbations in the rotational spectrum of conformer **I**. Selected transitions of **I** were fitted to a Hamiltonian allowing for this sort of interaction, and the separation between the two lowest vibrational states was determined to be  $58794(14)$  MHz [ $1.96112(5)$   $\text{cm}^{-1}$ ]. Attempts to include additional transitions in the fits using this Hamiltonian failed, and it is concluded that it lacks interaction terms to account satisfactorily for all the observed transitions. The situation was different for **II**. More than 2000 transitions were assigned and fitted to the usual Watson Hamiltonian, which allowed very accurate values to be determined not only for the rotational constants, but for many centrifugal distortion constants as well. Two vibrationally excited states were also assigned for this form. Theoretical calculations were performed at the B3LYP, MP2, and CCSD levels of theory using large basis sets to augment the experimental work. The predictions of these calculations turned out to be in good agreement with most experimental results.



## INTRODUCTION

The rotational spectrum of cyanoacetaldehyde ( $\text{NCCH}_2\text{CHO}$ ) has not previously been investigated. There are several reasons why the present investigation was undertaken. First, cyanoacetaldehyde may exist in the gas phase as a mixture of rotameric forms. Moreover, its tautomer, 3-hydroxy-2-propenenitrile (cyanovinylalcohol;  $\text{HOCH}=\text{CHCN}$ ), exists in equilibrium with cyanoacetaldehyde. In Figure 1, models of two conformers (denoted **I** and **II**) of cyanoacetaldehyde and three forms (**III**–**V**) of the tautomer cyanovinylalcohol are shown with atom numbering indicated on **I** and **III**.

The  $\text{C3}–\text{C1}–\text{C2}–\text{O4}$  dihedral angle can conveniently be used to define the conformational properties of cyanoacetaldehyde. Two rotameric forms may exist for this compound. The said dihedral angle turned out in the course of this work to be roughly  $150^\circ$  in **I**, halfway between anticlinal ( $120^\circ$ ; obsolete: gauche) and antiperiplanar ( $180^\circ$ ; obsolete: trans). This dihedral angle is  $0^\circ$  in **II**, which therefore takes a synperiplanar (obsolete: cis) conformation.

Received: December 21, 2011

Revised: March 20, 2012

Published: March 20, 2012

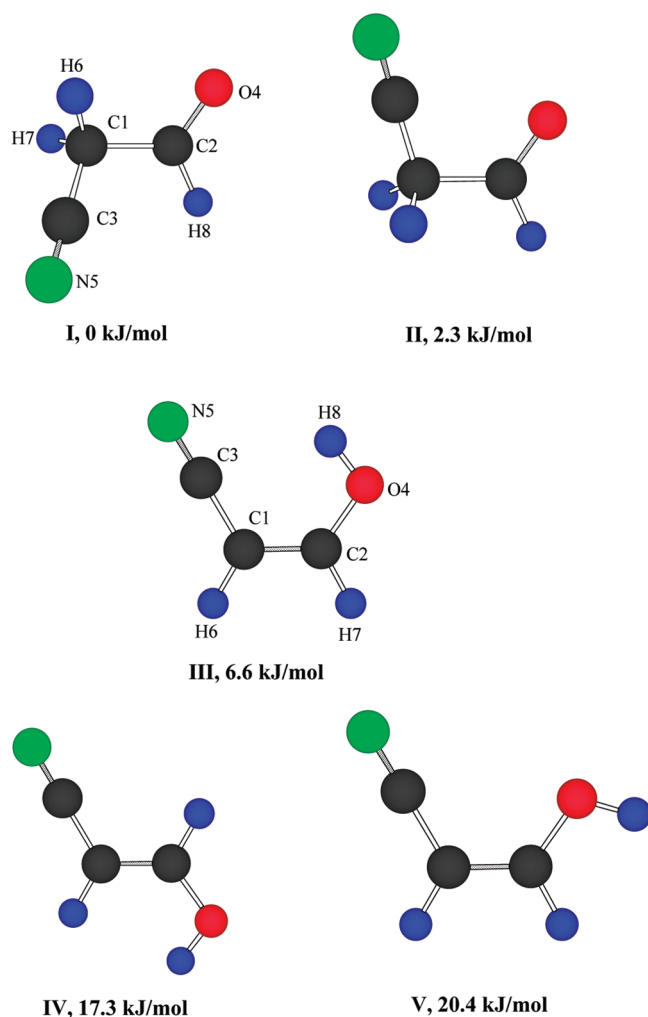


**Figure 1.** Conformers I and II are rotamers of cyanoacetaldehyde ( $\text{CH}_2(\text{CN})\text{CHO}$ ), whereas III–V are cyanovinylalcohol tautomers. Atom numbering is given on I and III. The MP2/aug-cc-pVTZ energy differences corrected for zero-point vibrational energies are given relative to the energy of I. Conformers I and II were found experimentally. Rotamer I was found to be 2.9(8) kJ/mol more stable than II by relative intensity measurements.

Cis and trans configurations exist for the tautomer cyanovinylalcohol. The cyano and alcohol groups are in a cis configuration in III and V, and in a trans configuration in IV. Rotation about the C2–O4 bond may result in rotational isomerism in each of the two tautomers. The three planar species III–V shown in Figure 1 represent typical forms of cyanovinylalcohol. It has been shown by NMR spectroscopy<sup>1</sup> that cyanoacetaldehyde predominates over cyanovinylalcohol in solution. Further forms of cyanovinylalcohol may exist, but they are likely to have even higher energies relative to I than conformers III–V. These very high-energy forms will consequently have extremely weak rotational spectra, and they have therefore not been considered further.

The synthesis of cyanoacetaldehyde is not straightforward. Hydrolysis of cyanoacetylene ( $\text{HC}\equiv\text{C}-\text{C}\equiv\text{N}$ ) in water leads to the formation of cyanoacetaldehyde,<sup>2</sup> but the problem is that it has not been possible to isolate cyanoacetaldehyde from the water solution. It is convenient, almost necessary, to use a neat sample in order to investigate a rotational spectrum. The first progress to isolate cyanoacetaldehyde was made by Claisen,

who already in 1903 reported a procedure for the opening of isoxazole by sodium ethylate followed by in situ trapping of the formed salt of cyanovinylalcohol.<sup>3</sup> The first isolation of cyanoacetaldehyde in an analytical scale was achieved in 1991 by flash vacuum thermolysis of a Meldrum acid derivative.<sup>4</sup> The mass spectrum of a crude mixture was obtained the following year.<sup>5</sup> Neat cyanoacetaldehyde, in sufficiently pure and in large enough quantities to allow a full spectroscopic study, was first prepared as recently as in 2007 by flash vacuum pyrolysis of isoxazole at 770 °C and isolated from impurities using a cold trap at –42 °C after the pyrolysis oven.<sup>1</sup> Cyanoacetaldehyde was found to be a moderately kinetically stable compound at room temperature and much more reactive than acetaldehyde.<sup>1</sup> Subsequent characterization by <sup>1</sup>H NMR spectroscopy of solutions of cyanoacetaldehyde showed the presence of both cyanoacetaldehyde and cyanovinylalcohol. The concentration of each of these tautomers was found to be strongly dependent on the solvent.<sup>1</sup>

It is interesting to note that the presence of a nitrile group in cyanoacetaldehyde makes the aldehyde form significantly more stable than the enol form, while the opposite is the case for the corresponding thiol and amine, which are vinyl derivatives, namely, *Z*- and *E*- $\text{HSCH}=\text{CHCN}$ ,<sup>6,7</sup> and *Z*- and *E*- $\text{H}_2\text{NCH}=\text{CHCN}$ ,<sup>8–10</sup> respectively. Microwave (MW) spectra of the *Z*-thiol<sup>7</sup> and the *Z*-amine<sup>10</sup> have already been reported.

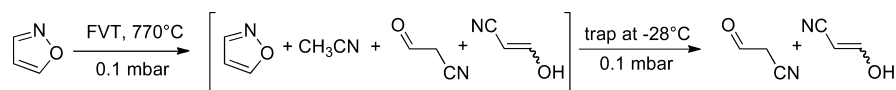
Rotational spectra have been used to identify the vast majority of molecules found in the interstellar medium.<sup>11,12</sup> Prebiotic existence of cyanoacetaldehyde is quite likely because of the facile hydrolysis of cyanoacetylene,<sup>2</sup> a compound that is formed in a spark discharge reaction in a methane–nitrogen mixture,<sup>13</sup> is prevalent in the interstellar medium,<sup>11</sup> and found in comets<sup>14</sup> and in Titan's atmosphere.<sup>15</sup> A gas-phase model of an uncatalyzed addition reaction between the two neutral molecules cyanoacetylene and water has been explored using quantum chemical calculations and found to be inefficient.<sup>16</sup> Protonated cyanoacetylene ( $\text{H}-\text{C}\equiv\text{C}-\text{C}\equiv\text{N}-\text{H}^+$ ) also exists in the interstellar medium.<sup>17</sup> The addition of water to this cation in the gas phase followed by an electron recombination reaction was also predicted to be inefficient but to a much lesser extent than the hydrolysis of cyanoacetylene.<sup>16</sup> The formation of cyanoacetaldehyde in liquid water, nevertheless, occurs,<sup>2</sup> presumably formed in a catalytic process.<sup>16</sup>

All this indicates that cyanoacetaldehyde may exist in the interstellar space or in planetary atmospheres. The title compound consists of eight atoms. Modern radio astronomy is now capable of detecting interstellar compounds of this complexity by means of their rotational spectra.<sup>11,12</sup> The rotational spectrum of cyanoacetaldehyde presented herein could therefore be the key for its identification anywhere in the Universe.

There is another important reason for performing a study of the rotational spectrum of cyanoacetaldehyde. The 1979 discovery of pyrimidines in the carbonaceous meteorites<sup>18</sup> showed that prebiotic synthesis of these important biomolecules, which are constituents of RNA and DNA, indeed occurs. Cyanoacetaldehyde has been demonstrated to react under various conditions with a number of likely prebiotic molecules to form pyrimidines, even in high yields.<sup>2,19–23</sup> This interesting potential prebiotic connection to pyrimidines should also be kept in mind.

Our experimental work has been augmented by high-level quantum chemical calculations, which were undertaken to obtain information for use in assigning the rotational spectrum

Scheme 1. Synthesis of Cyanoacetaldehyde



and investigating properties of the potential-energy hypersurface.

## EXPERIMENTAL SECTION

**Synthesis.** Cyanoacetaldehyde is a kinetically unstable compound at room temperature, and its revaporization is really challenging. The flash vacuum thermolysis at 770 °C under 0.1 mbar of isoxazole, a commercially available compound, led to the formation of cyanoacetaldehyde in a 24% yield. Selective trapping at −28 °C allowed us to obtain a pure compound (Scheme 1).<sup>1</sup> After several unsuccessful attempts to heat it as slowly as possible in vacuo (0.1 mbar) to have the lowest temperature of vaporization, we found that a more efficient way to vaporize it was a fast heating in a 50 °C water bath followed, when the expected vapor pressure was achieved, by a fast cooling with a liquid nitrogen bath to save the residual product. This unusual, but efficient, experiment was repeated up to 5 times with the same sample before the complete decomposition of the product. <sup>1</sup>H and <sup>13</sup>C NMR spectra of all the vaporized samples showed the presence of a pure product. We estimated that up to 20% of the compound can be revaporized under these conditions, where black oligomeric compounds were the main decomposition products.

**Spectroscopic Experiments in Oslo.** The MW spectrum of cyanoacetaldehyde was studied using the Stark-modulation MW spectrometer of the University of Oslo operating in the 7–120 GHz spectral range. Details of the construction and operation of this device have been given elsewhere.<sup>24–26</sup> This spectrometer has a resolution of about 0.5 MHz and measures the frequency of isolated transitions with an estimated accuracy of ~0.10 MHz. The 19.5–80.5 GHz frequency interval was recorded. Radio frequency microwave double-resonance experiments (RFMWDR), similar to those performed by Wodarczyk and Wilson,<sup>27</sup> were conducted to unambiguously assign particular transitions, using the equipment described elsewhere.<sup>24</sup> The sample, which was found to polymerize at room temperature, was kept at liquid-nitrogen (−196 °C) or dry ice temperature (−78.5 °C) when not in use. The ampule containing the sample had to be heated quickly at 50 °C with a water bath in order to fill the MW cell with a fresh portion, which was studied at a pressure of about 10 Pa. The formation of oligomeric brownish products was seen to occur during the heating of the sample.

**Spectroscopic Experiments in Lille.** The submillimeter-wave measurements (150–500 GHz) were performed employing the Lille spectrometer,<sup>28</sup> which is composed exclusively of solid-state devices as sources. The frequency of the Agilent synthesizer (12.5–17.5 GHz) was first multiplied by six and amplified by a Spacek active sextupler providing the output power of +15 dBm in the W-band range (75–110 GHz). This power is high enough to use passive Schottky multipliers (×2, ×3, and ×5) from Virginia Diodes Inc. in the next stage of the frequency multiplication chain. The detector is an InSb liquid He-cooled bolometer from QMC Instruments Ltd., which improves the sensitivity of the spectrometer. The sources were frequency modulated at 10 kHz. The absorption cell is a stainless-steel tube (6 cm diameter, 220 cm long). The

measurement accuracy for isolated lines is estimated to be better than 30 kHz. However, if the lines were blended or had a poor signal-to-noise ratio, their uncertainties were estimated to be 100 or even 200 kHz. The inverse squares of the uncertainties were used as weights in the least-squares fit of the spectrum. The line width was limited by Doppler broadening. The present measurements were performed at room temperature. The sample pressure during measurements was about 1.5 Pa (15 μbar). The filling of the cell was performed in the same way as in Oslo. We found that the sample was stable up to 7 h at this low pressure.

The Lille Fourier transform microwave spectrometer coupled to a pulsed molecular beam (MB-FTMW) was recently updated.<sup>29</sup> This device was used in an attempt to assign transitions of the two rotamers assigned in this work involving low values of the principal *J* quantum number. The sample was put in a reservoir, under a neon buffer gas pressure of 1 bar, and heated up to 50 °C. The *a*-type transitions of rotamer I were searched in the 5 GHz (1<sub>01</sub>–0<sub>00</sub> transition), 10 GHz (2<sub>02</sub>–1<sub>01</sub>), and 15 GHz (3<sub>03</sub>–2<sub>02</sub>) regions. Unfortunately, no signals were observed. This was probably due to the specific experimental conditions (i.e., long residual time in a heated reservoir) associated with the MB-FTMW spectrometer, which was not compatible with the chemical stability of cyanoacetaldehyde.

**Quantum Chemical Methods.** The present quantum chemical calculations were performed employing the Gaussian03 suite of programs,<sup>30</sup> running on the Titan cluster in Oslo. Becke's three-parameter hybrid functional<sup>31</sup> employing the Lee, Yang, and Parr correlation functional (B3LYP)<sup>32</sup> were employed in the density functional theory (DFT) calculations. Møller–Plesset second order perturbation theory (MP2) calculations<sup>33</sup> and coupled-cluster calculations with singlet and doublet excitations (CCSD)<sup>34,35</sup> were also undertaken. The CCSD calculations are very costly and were speeded up by making use of a B3LYP force field that was calculated prior to the CCSD calculations. Peterson and Dunning's<sup>36</sup> correlation-consistent aug-cc-pVTZ basis set, which is of triple-ζ quality and includes both diffuse and polarized functions, was used in the B3LYP and MP2 calculations. The smaller basis set cc-pVTZ<sup>36</sup> was employed in the CCSD calculations. This set does not include diffuse functions.

## RESULTS AND DISCUSSION

**Quantum Chemical Calculations.** MP2/aug-cc-pVTZ calculations were first performed in order to get an overview of which species might contribute significantly to the rotational spectrum. The fully optimized structures, dipole moments, and harmonic vibrational frequencies were calculated for conformers I and II of cyanoacetaldehyde and for the cyanovinylalcohol tautomers III–V depicted in Figure 1. Only positive vibrational frequencies were found for each species, which is indicative of a minimum (stable conformer) on the energy hypersurface. The results of these calculations are summarized in Tables 1S–5S of the Supporting Information.

It is seen from these tables that conformer I of cyanoacetaldehyde is calculated to be the global energy minimum of these five species. The MP2 energies of the



other forms relative to the energy of **I** are indicated on Figure 1. These values have been corrected for zero-point vibrational energies. Conformer **II** of cyanoacetaldehyde was found to have a symmetry plane with two out-of-plane hydrogen atoms ( $C_s$  symmetry). This conformer is predicted to be 2.3 kJ/mol less stable than **I**, while the cyanovinylalcohol species, **III**, is found to be 6.6 kJ/mol less stable and to be the lowest-energy forms of the three cyanovinylalcohol forms shown in this figure. This is consistent with the fact that **III** is stabilized by an internal hydrogen bond between the cyano and the hydroxyl group. Such stabilization is not possible for other forms of cyanovinylalcohol.

Rotamers **IV** and **V** are calculated to have significantly higher energies ( $\sim 17$ – $20$  kJ/mol) than **I**, and their rotational spectra are, for this reason, not considered further because they would presumably be extremely weak at room temperature.

The MP2 structures (Tables 1S–5S, Supporting Information) reveal no unusual structural parameters with one important exception, namely, the C3–C1–C2–O4 dihedral angle of conformer **I**. This dihedral angle is calculated to be  $144.9^\circ$ . This unusual angle deviates by about  $25^\circ$  from the canonical  $120^\circ$  angle, corresponding to an anticlinal conformation.

CCSD/cc-pVTZ calculations, which are at a much higher level of theory than MP2 calculations, were also undertaken. The CCSD method had to be restricted to the calculation of the energies of the optimized structures of **I** and **II**, their dipole moments, and their electronic field gradients, which allow the nuclear quadrupole coupling constants of the  $^{14}\text{N}$  nucleus to be calculated. Bailey's program AXIS<sup>30,37</sup> was used to transform the dipole moment components from the Gaussian03 standard orientation to the inertial principal-axis system, and his program NQC<sup>37</sup> was employed to calculate the principal-axis nuclear quadrupole coupling constants of the  $^{14}\text{N}$  nucleus.

The CCSD structures of **I** and **II** are listed in Table 1. Inspection of this table reveals that there are again no unusual bond lengths and bond angles in the two conformers except the C3–C1–C2–O4 dihedral angle of **I**, which is predicted to be  $147.2^\circ$  in this case. Conformer **II** was once more predicted to have  $C_s$  symmetry.

The rotational constants, the principal-axes dipole moments, and the nuclear quadrupole coupling constants are displayed in Table 2. This table also lists the planar moment,  $P_{\text{cc}}$ , defined by  $P_{\text{cc}} = 1/2(I_a + I_b - I_c)$ , where  $I_a$ ,  $I_b$ , and  $I_c$  are the principal moments of inertia, because its value is a sensitive indicator of the degree of nonplanarity. The CCSD electronic energy difference between **I** and **II** is 2.11 kJ/mol, again favoring **I** (Table 2).

DFT calculations generally require considerably less computational resources than MP2 or CCSD calculations, and this method has therefore been used to calculate a series of parameters that would otherwise require considerably more extensive calculations. The B3LYP method was used to calculate structures, energies, dipole moments, harmonic and anharmonic vibrational frequencies, Watson's  $A$ -reduction quartic and sextic centrifugal distortion constants,<sup>38</sup> and the vibration–rotation constants ( $\alpha$ ).<sup>39</sup>

The B3LYP structures of **I** and **II** are shown in Table 1. Interestingly, the C3–C1–C2–O4 dihedral angle of **I** was predicted to be  $150^\circ$  in this case. The B3LYP principal-axes dipole moments and electronic energy difference of 3.55 kJ/mol are displayed in Table 2. The energy difference becomes 3.71 kJ/mol after correction for zero-point vibrational energies.

**Table 1.** CCSD/cc-pVTZ and B3LYP/cc-pVTZ Structures of Conformers **I** and **II** of Cyanoacetaldehyde

method	CCSD		B3LYP	
conformer	I	II	I	II
Bond Length (pm)				
C1–C2	152.5	152.0	153.2	152.5
C1–C3	146.5	146.3	145.6	145.4
C1–H6	108.8	109.2	109.0	109.5
C1–H7	109.2	109.2	109.5	109.5
C2–O4	120.0	119.9	119.9	119.6
C2–H8	110.1	110.2	110.5	110.7
C3–N5	115.5	115.4	114.9	114.9
Angle (deg)				
C2–C1–C3	112.0	113.6	112.9	112.9
C2–C1–H6	109.2	108.5	108.9	107.9
C2–C1–H7	107.9	108.5	107.2	107.9
C3–C1–H6	110.8	109.7	111.1	110.0
C3–C1–H7	108.6	109.7	109.0	110.0
H6–C1–H7	108.2	106.6	107.5	105.8
C1–C2–O4	122.2	124.7	122.1	125.3
C1–C2–H8	115.8	113.6	115.7	114.9
O4–C2–H8	122.0	121.8	122.2	121.8
C1–C3–N5	178.2 <sup>a</sup>	178.8 <sup>b</sup>	178.0 <sup>a</sup>	179.1 <sup>b</sup>
Dihedral Angle (deg)				
C3–C1–C2–O4	–147.2	0.0	–150.1	0.0
C3–C1–C2–H8	34.3	180.0	31.3	180.0
H6–C1–C2–O4	–24.1	122.3	–26.1	123.0
H6–C1–C2–H8	157.4	–57.7	155.3	–56.9
H7–C1–C2–O4	93.3	–122.3	89.9	–123.0
H7–C1–C2–H8	–85.3	57.7	–88.7	56.9

<sup>a</sup>Bent toward H8. <sup>b</sup>Bent away from O4.

The harmonic and anharmonic vibrational frequencies of **I** are listed in Table 6S of the Supporting Information, whereas the vibrational frequencies of **II** are listed in Table 8S. The Watson quartic and sextic  $A$ -reduction centrifugal distortion constants<sup>38</sup> of conformer **II** are listed in Table 5. The vibration–rotation constants are shown in Tables 7S (conformer **I**) and Table 9S (**II**) of the Supporting Information.

The fact that the low-energy forms **I** and **II** are both conformers of cyanoacetaldehyde makes it of interest to explore the potential energy functions for rotation about the C1–C2 bond, which separates the two forms. Electronic energy potential functions were therefore calculated at both the MP2/aug-cc-pVTZ and B3LYP/aug-cc-pVTZ levels of theory employing the scan option of Gaussian03. The energies were computed in steps of  $10^\circ$  of the C3–C1–C2–O4 dihedral angle. All the remaining structural parameters were optimized for each dihedral angle. Separate calculations of the energies and optimized structures of the transition states near  $60^\circ$  and at  $180^\circ$  were also performed. The potential functions (red circles, MP2; blue squares, B3LYP) based on the results of these calculations combined with the above results for **I** and **II** are drawn in Figure 2. The global minimum (conformer **I**) has a C3–C1–C2–O4 dihedral angle of  $145^\circ$  (MP2) and  $150^\circ$  (B3LYP). The second minimum at  $0^\circ$  found in both methods corresponds to conformer **II**. The electronic energy differences between **I** and **II** are 2.33 (MP2) and 3.55 kJ/mol (B3LYP). The energy of the transition state at  $61^\circ$  are 9.66 (MP2) and 10.59 kJ/mol (B3LYP), respectively.

Most interestingly, both methods predict very low values for the second transition state at the exact antiperiplanar ( $180^\circ$ )

**Table 2. CCSD/cc-pVTZ and B3LYP/cc-pVTZ Spectroscopic Constants of Conformers I and II of Cyanoacetaldehyde**

method	CCSD		B3LYP	
conformer	I	II	I	II
Rotational Constants (MHz)				
A	26 034.6	12 886.2	26 933.0	13 111.8
B	2584.7	3643.4	2569.6	3579.8
C	2438.9	2890.5	2425.1	2861.0
CCSD Planar Moment ( $10^{-20}$ u m <sup>2</sup> )				
$P_{cc}^a$	3.86	1.55	4.60	1.54
Dipole Moment <sup>b</sup> ( $10^{-30}$ C m)				
$\mu_a$	3.11	8.98	3.77	8.13
$\mu_b$	5.25	16.95	4.94	15.51
$\mu_c$	4.25	0.0 <sup>c</sup>	3.43	0.0 <sup>c</sup>
$\mu_{tot}$	7.44	19.18	7.10	17.51
Quadrupole Coupling Constant <sup>d</sup> (MHz)				
$\chi_{aa}$	−3.600	−2.399		
$\chi_{bb}$	1.239	−0.097		
$\chi_{ab}$	3.036	3.664		
Electronic Energy Difference Relative to I (kJ/mol)				
$\Delta E$	0.0 <sup>e</sup>	2.11	0.0 <sup>f</sup>	3.55 <sup>g</sup>

<sup>a</sup>Planar moment defined by  $P_{cc} = 1/2(I_a + I_b - I_c)$ , where  $I_a$ ,  $I_b$ , and  $I_c$  are the principal moments of inertia. Conversion factor:  $505379.05 \times 10^{-20}$  MHz u m<sup>2</sup>. <sup>b</sup>One debye =  $3.33564 \times 10^{-30}$  C m. <sup>c</sup>For symmetry reasons. <sup>d</sup>The nuclear quadrupole coupling constants of the nitrogen nucleus were calculated only at the CCSD level of theory. <sup>e</sup>CCSD electronic energy of I: −644897.81 kJ/mol. <sup>f</sup>B3LYP electronic energy of I: −646294.48 kJ/mol. <sup>g</sup>The energy difference becomes 3.71 kJ/mol when corrected for zero-point vibrational energies.

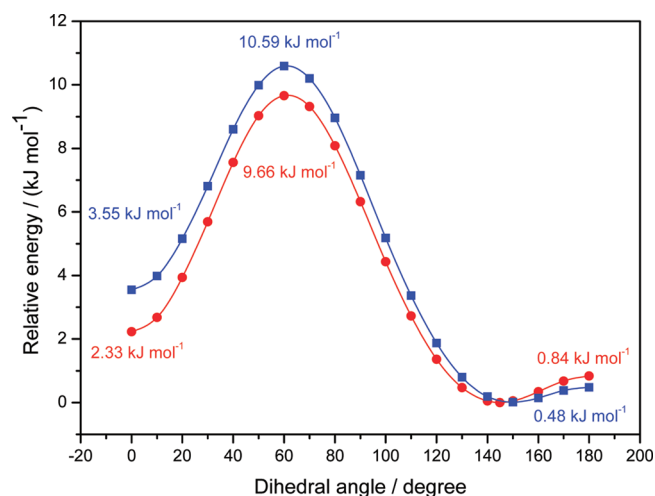


**Figure 2.** MP2/aug-cc-pVTZ (red, circles) and B3LYP/aug-cc-pVTZ (blue, squares) electronic energy potential functions for rotation about the C1–C2 bond of cyanoacetaldehyde. The C3–C1–C2–O4 dihedral angles are given on the abscissa, and the energies relative to the global-minimum, conformer I, are given on the ordinate.

conformation. MP2 indicates 0.84, while B3LYP yields 0.48 kJ/mol for this barrier height.

A double-minimum potential for rotation about the C1–C2 bond with a comparatively small barrier at the exact antiperiplanar conformation is therefore predicted to exist for this compound. A barrier of this height should lead to large-amplitude vibrations for the torsion about the C1–C2 bond and to two closely spaced energy levels for the ground

vibrational state of conformer I. These energy levels are often designated with a (+) for the lowest-energy level and a (−) for the higher-energy level. Moreover, coupling between vibration and rotation is often observed in such low-barrier cases, often resulting in complicated rotational spectra that cannot be fitted satisfactorily to the standard Watson Hamiltonian,<sup>38</sup> which does not take this effect into account. Complicated vibration–rotation coupling was indeed found to be a prominent perturbation in the rotational spectrum of I (see below).

Quantum chemical model calculations are often a very useful aid for the assignment of rotational spectra complicated by vibration–rotation coupling. Recently, such calculations were successfully performed for thiophenol and 4-fluorothiophenol,<sup>40</sup> which present similar problems as that of I, associated with the large-amplitude vibration of the thiol groups in these two compounds. It was therefore decided to undertake a similar modeling for I, using the same method.<sup>40</sup> This procedure<sup>40</sup> combines an internal rotation program called SEMIRIG with the program ASMJS. The latter computer program fits vibration–rotation energy levels for  $J \leq 7$  to rotational and centrifugal distortion constants as well as Coriolis coupling constants for two closely spaced vibrational levels.<sup>40</sup> The SEMIRIG program has the internal rotation of one part of the molecule, the CH<sub>2</sub>(CN) group in our case, against the other part, the CHO group, as the only internal degree of freedom and has no symmetry restriction on the two parts of the molecule. A detailed account of this program has been published.<sup>41</sup>

The internal rotation potential function in SEMIRIG has the form  $V(\gamma) = \Sigma 1/2V_n(1 - \cos(n\gamma))$ , where  $\gamma$  is the internal rotation angle. Only the first three coefficients of this expansion,  $V_1$ – $V_3$ , were employed in the present calculations. Their values, which are listed in Table 3, were obtained from the B3LYP potential function shown in Figure 2, making use of the minima at 0 and 150° and the maximum at 61°. Necessary

**Table 3. Potential Constants, Mean Rotational Constants, Energy Difference, and Coupling Constants of Conformer I of Cyanoacetaldehyde**

	B3LYP <sup>a</sup>	Exp. <sup>b</sup>
Potential Constants <sup>c</sup> (kJ/mol)		
$V_1$	−7.864	
$V_2$	5.141	
$V_3$	5.143	
Mean Rotational Constants <sup>d</sup> (MHz)		
$A_m$	26 727.27	26 749.46
$B_m$	2569.11	2577.69
$C_m$	2434.63	2425.08
Difference between the Rotational Constants of the Two States (MHz)		
$\Delta A$	−429.25	−14.66
$\Delta B$	5.66	3.39
$\Delta C$	7.93	3.02
Planar Moment ( $10^{-20}$ u m <sup>2</sup> )		
$P_{cc}$	4.02	3.28
Difference between the (+)- and (−)-States (MHz)		
$\Delta E$	68158	58794
Coriolis Coupling Constants (MHz)		
$F_{bc}$	9.8	0.52
$F_{ac}$	11.0	0.0 <sup>c</sup>

<sup>a</sup>The rotational constants have been obtained in the combined B3LYP plus SEMIRIG-ASMJS calculations. <sup>b</sup>See text. <sup>c</sup>Fit 1, Table 4. <sup>d</sup>Fixed.

structural parameters were taken from the B3LYP structure of **I** (Table 1). All rotational levels with  $J \leq 7$  of the (+)- and (-)-states were fitted precisely by ASMJ5 to obtain effective rotational constants, plus centrifugal distortion constants of both states, as well as the  $F_{bc}$  and  $F_{ac}$  Coriolis coupling constants of the two states. The (+)- and (-)-levels were calculated in this manner to be spaced by 68 158 GHz (about  $2.27 \text{ cm}^{-1}$ ); see Table 3. In the same table, the mean values of the rotational constants of the (+)- and (-)-states are shown together with the differences between the upper (-)-state and the lower (+)-state rotational constants. The B3LYP rotational constants in Table 3, referring to the ground-vibrational state, differ a little from their counterparts in Table 2, which refer to the approximate equilibrium structure. The quartic centrifugal distortion constants based on the B3LYP plus SEMIRIG ASMJ5 model calculations were  $\Delta_J = 0.88$ ,  $\Delta_{JK} = -102$ ,  $\Delta_K = 3191$ ,  $\delta_J = -0.138$ , and  $\delta_K = 1.7 \text{ kHz}$  for the (+)-state, remarkably different from the corresponding constants for the (-)-state, which were 0.63, -68, 2027, -0.088, and -7.2 kHz, respectively.

**Microwave Spectrum and Assignment of **I**.** Conformer **I** is predicted in the theoretical calculations above to be preferred over **II** by 2–4 kJ/mol and over **III** by 6.6 kJ/mol. **I** and **II** might be present in so high concentrations that it should be possible to assign their rotational spectra, while **III** presumably has a small Boltzmann factor at room temperature and has consequently a very weak spectrum, which would probably be difficult to assign. It was therefore initially assumed that the spectra of **I** and **II** would be responsible for the vast majority of the observed absorption lines. Both these rotamers are prolate and have their major dipole moment component along the  $b$  axis (Table 2). The perpendicular  $b$ -type spectra of prolate rotors are rich, and this was indeed observed as the rotation spectrum was found to have absorption lines occurring every few megahertz throughout the investigated spectral ranges.

The  $K_{-1} = 1 \leftarrow 0$   $b$ -type  $Q$ -branch transitions of the spectrum of **I** were predicted to be among the strongest lines of the spectrum. Searches were first undertaken in Oslo for these transitions using the spectroscopic constants of Table 1 to predict their approximate spectral frequencies. These transitions were soon identified. Most interestingly, these lines appeared as doublets of apparently equal intensities and were generally separated by several megahertz. Calculation of the  $^{14}\text{N}$  nucleus quadrupole splittings of these transitions using program MB09<sup>42</sup> and the nuclear quadrupole coupling constants of Table 2 revealed that the doublets could not at all be explained by this effect, which would cause relatively small and only partly resolved splittings of the strongest quadrupole components. However, this doublet feature and the existence of (+)- and (-)-states is exactly what the calculations above predict for a compound possessing a double-minimum potential with a small barrier maximum at the antiperiplanar position.

The  $K_{-1} = 1 \leftarrow 0$   $b$ Q lines of both the (+)- and the (-)-state could be fitted reasonably well to Watson's Hamiltonian<sup>38</sup> in the  $A$ -reduction  $F$ -representation using Sørensen's program ROTFIT.<sup>43</sup> The fact that the  $A$  rotational constant is larger for the (+)-state than for the (-)-state, whereas the opposite is the case for  $B$  and  $C$ , is in accord with the B3LYP calculations (Table 3). This criterion was used to assign the observed spectra to the (+)- and (-)-states and not vice versa.

The preliminary spectroscopic constants obtained from these first  $Q$ -branch transitions were used to predict the next  $Q$ -

branch series, where  $K_{-1} = 2 \leftarrow 1$ . Many of these transitions were readily assigned because their frequencies were close to those predicted using the Watson Hamiltonian.<sup>38</sup> However, some of these transitions were definitely shifted from the frequencies predicted using this Hamiltonian, and Coriolis coupling between vibration and rotation was suspected of causing this inconsistency.

Having assigned the  $b$ Q-lines, when possible, the assignment of  $a$ -type  $R$ -branch lines became the next target. The  $K_{-1} \geq 3$   $a$ R-branch lines occur in pile-ups because **I** is a very prolate rotor with Ray's asymmetry parameter<sup>44</sup>  $\kappa \approx -0.99$ . These transitions are modulated at comparatively low Stark field strengths, which makes them easy to assign, and are often good candidates for the very specific RFMWDR method. The result of a RFMWDR search is shown in Figure 3. It is seen from this

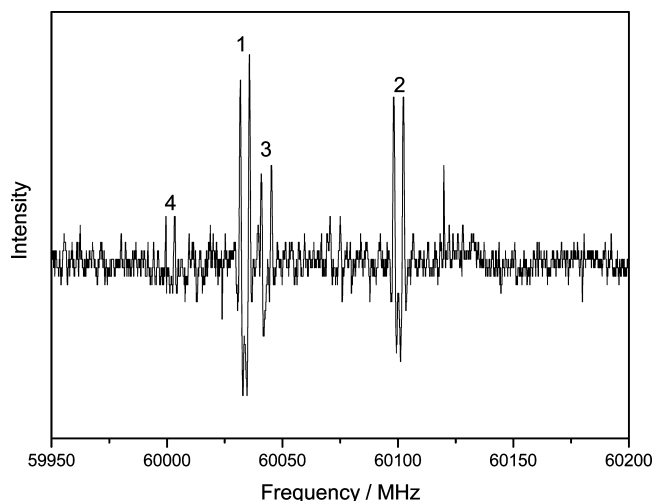


**Figure 3.** Portion of the RFMWDR spectrum of the  $J = 12 \leftarrow 11$  transition obtained employing a radio frequency of 7.50 MHz. The spectrum shows the  $J = 12_3 \leftarrow 11_3$  pair of lines of four vibrational states. The state denoted 1 is assumed to be the (+)-state, and the state denoted 2 is assumed to be the (-)-state. The states denoted 3 and 4 are other vibrationally excited states, which were not analyzed further.

figure that the (+)- and the (-)-states have roughly the same intensity, which is expected for two closely spaced energy levels with a separation of a few  $\text{cm}^{-1}$ .

Inclusion of  $a$ R-branch transitions together with the  $b$ Q-lines in the least-squares procedure of ROTFIT allowed preliminary values of spectroscopic constants to be calculated and further  $b$ -type  $R$ -branch lines to be assigned as the next step.

These constants were used to predict the millimeter-wave spectrum with the Watson Hamiltonian.<sup>38</sup> This allowed many additional transitions to be assigned in Lille. Interestingly, transitions up to  $J = 40$  and  $K_{-1} = 7$  of the (-)-state could be fitted satisfactorily to this Hamiltonian. However, many lines of the (+)-state were definitely perturbed and a more elaborate Hamiltonian than Watson's was needed to produce a better fit.

A Hamiltonian, which includes Coriolis coupling similar to the one used successfully for ethanetellurol,<sup>45</sup> seemed to be a natural choice. The Hamiltonian<sup>40</sup> we employed, includes a coupling between the two states of the type  $F_{bc}(\hat{J}_b \hat{J}_c + \hat{J} \hat{J}_b)$ . This procedure gave a very good fit to low- $K_{-1}$  lines ( $K_{-1} < 3$ ), and it was even possible to include a number of lines, which did not fit to Watson's Hamiltonian. These strongly perturbed lines all belonged to the (+)-state. The spectrum consisting of 199



transitions from the 19.5–80 GHz spectral region with  $K_{-1} < 3$  is listed in Table 10S of the Supporting Information. The spectroscopic constants obtained from this fit, denoted fit 1, are listed in the second column of Table 4. The mean values of the

**Table 4. Spectroscopic Constants<sup>a</sup> of Conformer I of Cyanoacetaldehyde**

fit no.	1	2	3
(+)–State			
A (MHz)	26 756.77(9)	26 756.67(12)	
B (MHz)	2576.000(4)	2575.982(5)	
C (MHz)	2423.565(6)	2423.562(8)	
$\Delta_J$ (kHz)	1.431(17)	1.348(21)	
$\Delta_{JK}$ (kHz)	−98.9(6)	−100.8(8)	
$\Delta_K$ (kHz)	2635(20)	2628(26)	
$\delta_J$ (kHz)	0.035(6)	0.046(8)	
$\delta_K$ (kHz)	−4.9(14)	−8.5(20)	
$\Phi_J$ (Hz)	0.08(2)	−0.07(3)	
$\Phi_{JK}$ (Hz)	20.1(8)	15.3(10)	
$\Phi_{KJ}$ (Hz)	1288(135)	1067(173)	
$\phi_J$ (Hz)	−0.017(6)	−0.0002(80)	
$\phi_{JK}$ (Hz)	−50(4)	−38(5)	
$\lambda_{JK}$ (mHz)	23(3)	12(4)	
(−)–State			
A (MHz)	26 742.13(8)	26 741.75(7)	26 742.006(22)
B (MHz)	2579.388(4)	2579.3959(20)	2579.3873(10)
C (MHz)	2426.588(4)	2426.5975(22)	2426.5878(11)
$\Delta_J$ (kHz)	0.911(15)	0.9291(21)	0.9232(9)
$\Delta_{JK}$ (kHz)	−35.4(4)	−36.17(8)	−36.557(29)
$\Delta_K$ (kHz)	394(16)	299(17)	361(5)
$\delta_J$ (kHz)	0.1354(2)	0.1426(14)	−0.1349(3)
$\delta_K$ (kHz)	−22.0(3)	−23.49(23)	22.33(12)
$\Phi_J$ (Hz)	−0.013(14)	−0.0002(7)	−0.0012(3)
$\Phi_{JK}$ (Hz)	−0.66(23)	1.04(8)	0.764(10)
$\Phi_{KJ}$ (Hz)	321(96)	−60(3)	−68.3(16)
$\Phi_K$ (Hz)		−790(762)	1812(201)
$\phi_J$ (Hz)		0.0111(15)	−0.0019(1)
$\phi_{JK}$ (Hz)		−2.12(16)	1.53(9)
$\Lambda_{JK}$ (mHz)		−0.042(28)	
$\Lambda_{JK}$ (mHz)		−2.9(9)	
$\Lambda_{KK}$ (mHz)		195(43)	217(23)
$\lambda_K$ (mHz)		−0.0028(5)	
Coupling Terms			
$\Delta$ (MHz)	58 794(14)	58 735(17)	
$G_c^b$ (MHz)		0.74(22)	
$F_{bc}^c$ (MHz)	0.5208(15)	1.13(3)	
$h_{xyj}^d$ (kHz)		−0.74(4)	
rms <sup>e</sup> (kHz)	0.156	0.204	0.123
no. of lines	199	413	316

<sup>a</sup>See text. Uncertainties represent one standard deviation. <sup>b</sup>Operator:  $\hat{J}_c$ . <sup>c</sup>Operator:  $(\hat{J}_b\hat{J}_c + \hat{J}_c\hat{J}_b)$ . <sup>d</sup>Operator:  $(\hat{J}_b\hat{J}_c + \hat{J}_c\hat{J}_b)^2$ . <sup>e</sup>Root-mean-square deviation.

rotational constants of the (+)- and (−)-states are shown in Table 3 together with the B3LYP counterparts.

The agreement between the experimental and B3LYP rotational constants is remarkable, the main difference being much larger than observed values for  $\Delta A$ . The theoretical coupling constants  $F_{bc}$  and  $F_{ac}$  are much larger than their experimental counterparts (Table 3). The quartic centrifugal distortion constants given in the text above differ much from the experimental values shown in Table 4. This is expected

since the only internal degree of freedom in the model calculations is the torsion about the C1–C2 bond.

More unexpected is maybe the large differences between the experimental centrifugal distortion constants from the (+) to the (−) state (Table 4), but since also the model calculations give large differences between the two states, we suggest that the differences are caused primarily by the highly anharmonic potential function with many low-lying torsional states.

The separation between the (+)- and (−)-energy levels was found to be 58 794(14) MHz [ $1.96112(5) \text{ cm}^{-1}$ ] in fit 1 (Table 4), compared to the B3LYP value of 68 158 MHz (Table 3), which is considered to be satisfactory.

In a second least-squares fit, called fit 2, a total of 413 lines listed in Table 11S, Supporting Information, were fitted. Transitions from the (+)-state with  $K_{-1} < 3$  and lines from the (−)-state with  $K_{-1} < 8$  were employed in this fit. The (+)-state lines are from the 20–80 GHz spectral interval. Several inconsistencies were observed when (+)-state lines from the region above 150 GHz were included in the fit, and no such lines were therefore used to obtain the spectroscopic constants shown in Table 4. However, many (−)-state transitions from the high-frequency spectral interval have been used (Table 11S, Supporting Information). In order to obtain this fit, lines involving rotational levels of the type  $J_{1J}$  with  $J = 30, 31$ , and  $32$  had to be excluded. Even though three different coupling operators were used, lines involving these levels were not well reproduced by the fit. The most disturbing fact is that most of the lines in the upper state can be fitted pretty well to a usual Watson Hamiltonian, as shown in fit 3 of Table 4.

Altogether, we consider fit 1 to be best, but the cause of the problems or inconsistencies encountered is not known. It might be due to some wrong assignments or the reason could be that an unknown third state is involved. Finally, and most likely, the effective Hamiltonian used is not adequate and lacks some kind of operator or coupling to other states.

The (+)- and (−)-states are separated by 58 794(14) MHz according to fit 1. The  $c$ -type transitions should occur between these two levels. It is seen from Table 2 that rather significant values of  $\mu_c$  are predicted in the theoretical calculations for conformer I. Searches were therefore undertaken in an attempt to assign  $c$ -type transitions using the separation by about 58 794 MHz to guide the efforts. However, no  $c$ -type lines could be assigned in this dense spectrum in this manner.

**Assignment of the Spectrum of II.** The theoretical calculations above (Figure 1 and Table 2) indicate that rotamer II should be 2–4 kJ/mol less stable than I. This high-energy rotamer of cyanoacetaldehyde is predicted to have a comparatively large  $\mu_b$  of about  $17 \times 10^{-30} \text{ C m}$  (CCSD value; Table 2), and it should therefore have a relatively strong  $b$ -type spectrum even given an energy difference of a few kJ/mol. Successful searches for  $^bQ$ -branch transitions were first performed in Oslo using the CCSD rotational constants (Table 2) and the B3LYP centrifugal distortion constants (Table 5) to predict their approximate frequencies. The assignments were then extended to include additional  $b$ -type  $Q$ - and  $R$ -branch lines, as well as  $^aR$ -transitions.

Using the preliminary spectroscopic constants from the Oslo measurements, the assignments of the millimeter and submillimeter-wave spectra were fairly easy to perform. The major difficulty came from the high density of the spectra due to unassigned lines from excited vibrational states of conformer I. Hundreds of lines from the first excited state of the lowest

Table 5. Spectroscopic Constants<sup>a</sup> of Conformer II of Cyanoacetaldehyde

vibrational state	ground	first torsion	first bending	equilibrium <sup>b</sup>
A (MHz)	12 812.11068(26)	12 790.675(14)	12 923.719(19)	12 886.2
B (MHz)	3658.693685(84)	3638.8267(62)	3671.230(10)	3643.4
C (MHz)	2894.587294(87)	2895.3248(62)	2894.104(10)	2890.5
$P_{cc}$ ( $10^{-20}$ u m <sup>2</sup> )	1.490958(6)	1.9234(1)	1.0702(1)	1.545
$\Delta_J$ (kHz)	3.533884(54)	3.266(29)	3.692(38)	3.21
$\Delta_{JK}$ (kHz)	−24.99519(19)	−24.079(60)	−25.602(79)	−22.8
$\Delta_K$ (kHz)	84.6528(17)	79.48(16)	93.29(80)	84.1
$\delta_J$ (kHz)	1.079689(20)	1.0094(15)	1.1408(17)	0.950
$\delta_K$ (kHz)	6.95591(91)	1.312(70)	12.044(74)	6.78
$\Phi_J$ (Hz)	0.011740(15)	−0.113(13)		0.00427
$\Phi_{JK}$ (Hz)	−0.003236(95)	−0.080(65) <sup>c</sup>	0.452(71) <sup>c</sup>	−0.0170
$\Phi_{KJ}$ (Hz)	−0.54216(30)			−0.413
$\Phi_K$ (Hz)	2.0026(48)			1.81
$\phi_J$ (Hz)	0.0052897(62)			0.00427
$\phi_{JK}$ (Hz)	0.01755(74)			0.0143
$\phi_K$ (Hz)	1.07672(85)			0.986
$\Lambda_J$ (mHz)	−0.0000470(13)			
$\Lambda_{JK}$ (mHz)	0.0000268(82)			
$\Lambda_{JK}$ (mHz)	−0.004269(43)			
$\Lambda_{KJ}$ (mHz)	0.02444(22)			
$\Lambda_K$ (mHz)	−0.0677(41)			
$\lambda_J$ (mHz)	−0.00001837(57)			
$\lambda_{JK}$ (mHz)	0.00175(19)			
$\pi_{JK}$ ( $\mu$ Hz)	−0.000137(16)			
rms <sup>d</sup>	0.921	1.709	1.474	
no. of lines <sup>e</sup>	2338	104	78	

<sup>a</sup>A-reduction.<sup>38</sup> Uncertainties represent one standard deviation. <sup>b</sup>CCSD rotational constants and B3LYP centrifugal distortion constants. <sup>c</sup>Further centrifugal distortion constants preset at zero. <sup>d</sup>Weighted root-mean-square deviation. <sup>e</sup>Number of lines used in the least-squares fit.

bending vibration of this conformer could be assigned in the millimeter-wave spectra.

A total of 2338 lines shown in Table 13S, Supporting Information, were used to calculate the spectroscopic constants of the ground vibrational state of rotamer II. These parameters, which are listed in Table 5, were obtained in a weighted least-squares fit employing the computer program ASFIT.<sup>46</sup> It is seen from Table 5 that very accurate values have been obtained not only for the rotational constants but also for the quartic and sextic centrifugal distortion constants. The experimental quartic centrifugal distortion constants agree with the B3LYP constants to within about 10% or better, while much larger discrepancies exist for some of the sextic constants.

**Vibrationally Excited State of II.** There exist two low-frequency vibrational normal modes of this rotamer with harmonic frequencies at 134 and 156 cm<sup>−1</sup>, according to the B3LYP calculations shown in the Supporting Information, Table 8S. The former of these modes is the torsion about the C1–C2 bond, whereas the latter is the lowest bending vibration. A total of 104 transitions were assigned for the spectrum of the first excited state of the torsion and 78 lines were assigned for the first excited state of the lowest bending vibration. These spectra are listed in Tables 14S and 15S of the Supporting Information, while the spectroscopic constants obtained in a weighted least-squares calculation using ROTFIT<sup>43</sup> are shown in Table 5.

It is seen from this table that the planar moment,  $P_{cc}$ , increases for the first excited state of the torsion compared with the ground vibrational state. This is typical for an out-of-symmetry-plane vibration.<sup>47,48</sup> Relative intensity measurements performed largely as described by Esbitt and Wilson<sup>49</sup> yielded

126(25) cm<sup>−1</sup> for this vibration, in good agreement with the B3LYP harmonic value, 134 cm<sup>−1</sup>.

The vibration–rotation constants,<sup>39</sup>  $\alpha$ , calculated from  $\alpha = X_0 - X_1$ , where  $X_0$  is a rotational constant of the ground vibrational state and  $X_1$  is a rotational constant of the first excited state of the normal mode in question, were calculated from the entries of Table 5 as  $\alpha_A = 21.43$ ,  $\alpha_B = 19.86$ , and  $\alpha_C = -0.74$  MHz, respectively. This is in fair agreement with the B3LYP values (Table 9S, Supporting Information), which are  $\alpha_A = 39.32$ ,  $\alpha_B = 17.09$ , and  $\alpha_C = -1.36$  MHz.

Relative intensity measurements<sup>49</sup> yielded 158(30) cm<sup>−1</sup> for the first excited state of the in-symmetry-plane bending vibration, close to the B3LYP prediction of 156 cm<sup>−1</sup>.  $P_{cc}$  decreases for this excited state compared to the ground vibrational state (Table 5), which is in accord with theory.<sup>47,48</sup> The vibration–rotation constants obtained from the values in Table 5 are  $\alpha_A = -111.61$ ,  $\alpha_B = -12.54$ , and  $\alpha_C = 0.48$  MHz, compared to the B3LYP values (Table 9S, Supporting Information) of  $\alpha_A = -125.63$ ,  $\alpha_B = -13.25$ , and  $\alpha_C = 0.62$  MHz, respectively. The agreement is again satisfactory.

**Searches for the Tautomer III.** This species is comparatively polar with MP2 dipole moment components of  $\mu_a \approx 10$ , and  $\mu_b \approx 6.5 \times 10^{-30}$  C m (Table 3S, Supporting Information). The rather large energy difference of 6.6 kJ/mol (Figure 1) between this form and conformer I indicates that it would possess a small Boltzmann factor at room temperature and, consequently, that the spectrum would be expected to be very weak. Extensive searches for this spectrum were made using the MP2 rotational constants and dipole moment components (Table 3S, Supporting Information) to predict



the spectrum, but no assignments were achieved, presumably because of its weakness.

**Energy Difference between I and II.** The energy difference between I and II was determined from relative intensity measurements observing the precautions of Esbitt and Wilson.<sup>49</sup> Several selected transitions of both conformers were used. The internal energy difference between the ground states of the two forms was calculated as described by Townes and Schawlow.<sup>50</sup> The result was 2.9(8) kJ/mol, with I as the lowest-energy conformer. There are several sources of error involved in relative intensity measurements,<sup>49</sup> and a liberal uncertainty limit is estimated to be  $\pm 0.8$  kJ/mol. The energy difference of 2.9(8) kJ/mol should be compared to the theoretical results, which are 2.3 (MP2), 3.7 (B3LYP), and 2.1 kJ/mol (CCSD), demonstrating good agreement with experiment.

**Structures.** It is our experience that CCSD/cc-pVTZ bond lengths and bond angles of molecules such as cyanoacetaldehyde are very close to the equilibrium values. The bond lengths and bond angles of conformer I given in Table 1 are therefore assumed to be our best estimates of these equilibrium parameters.

A different situation exists for the value of the C3–C1–C2–O4 dihedral angle, which is of major interest in the case of conformer I. Figure 1 indicates that the potential curve is rather flat around 150°. The accurate value of the true minimum of this curve can therefore be difficult to obtain in the theoretical calculations.

The C3–C1–C2–O4 dihedral angle is very sensitive to the value of the planar moment,  $P_{cc}$ . The experimental value is  $3.28 \times 10^{-20}$  u m<sup>2</sup> (Table 3), compared to 4.02 (B3LYP; Table 3), 4.19 (MP2, calculated from the entries in Table 1S, Supporting Information), and 3.86 (CCSD; Table 2). All three theoretical values are therefore too large, which indicates that the theoretical values of the C3–C1–C2–O4 dihedral angle, which were 150 (B3LYP), 145 (MP2), and 147° (CCSD), are slightly too small.

An improved value of the C3–C1–C2–O4 dihedral angle was obtained by rotating about the C1–C2 bond keeping the bond length and bond angles fixed at the CCSD values shown in Table 1. A value of 151° for the C3–C1–C2–O4 dihedral angle yielded  $P_{cc} = 3.40 \times 10^{-20}$  u m<sup>2</sup>, in good agreement with the experimental value of  $3.28 \times 10^{-20}$  u m<sup>2</sup> (Table 3). The rotational constants obtained in this manner are  $A = 26\,764.2$ ,  $B = 2574.0$ , and  $C = 2424.8$  MHz, which compares very well with the experimental results shown in Table 3. The uncertainty limit of the C3–C1–C2–O4 dihedral angle of conformer I is estimated to be  $\pm 3^\circ$ .

The situation for conformer II is simpler than that for I. Inspection of Table 5 reveals that there is very good agreement between the ground-state rotational constants (column 2) and the CCSD rotational constants (column 5, Table 2) calculated from the structure in Table 1. The CCSD structure is an approximation of the equilibrium structure, while the experimental rotational constants reflect the effective structure ( $r_0$  structure), which is defined differently. Nevertheless, the good agreement between the experimental and CCSD rotational constants indicates that the CCSD structure is indeed close to the equilibrium structure.

## CONCLUSIONS

The present study has shown that cyanoacetaldehyde (NCCH<sub>2</sub>CHO) is strongly preferred over its tautomer cyanovinylalcohol (NCCH=CHOH) in the gas phase. The

spectra of two rotameric forms of cyanoacetaldehyde produced by rotation about the C–C bond have been assigned. The cyano and carbonyl groups forms an unusual angle of 151(3)° from the synperiplanar (0°) position in I. These groups are exactly synperiplanar in II. Conformer I is preferred over II by 2.9(8) kJ/mol.

A double minimum potential for rotation about the C–C bond with a small barrier maximum at the exact anticlinal (180°) leads to Coriolis perturbations in the rotational spectrum of conformer I. Selected transitions of the spectrum of I was fitted to a Hamiltonian allowing for this sort of interaction and the separation between the two lowest vibrational states were determined to be 58 794(14) MHz [ $1.96112(5)$  cm<sup>−1</sup>]. However, attempts to include additional transitions in the fits using this Hamiltonian failed, and it is concluded that it lacks interaction terms to account satisfactorily for all the observed transitions.

The Coriolis perturbation appears to be limited to conformer I because more than 2000 transitions were assigned and fitted to the usual Watson Hamiltonian. This large number of transitions yielded very accurate values not only for the rotational constants but also for many centrifugal distortion constants. Two vibrationally excited states were also assigned for this form, and their vibrational frequencies were determined by relative intensity measurements.

Theoretical calculations were performed at the B3LYP, MP2, and CCSD levels of theory using large basis sets to augment the experimental work. The predictions of these calculations turned out to be in good agreement with most of the experimental results, when a comparison could be made.

## ASSOCIATED CONTENT

### Supporting Information

Results of the theoretical calculations and the microwave spectra. This material is available free of charge via the Internet at <http://pubs.acs.org>.

## AUTHOR INFORMATION

### Corresponding Author

\*Tel: +47 2285 5674. Fax: +47 2285 5441. E-mail: [harald.mollendal@kjemi.uio.no](mailto:harald.mollendal@kjemi.uio.no).

### Notes

The authors declare no competing financial interest.

## ACKNOWLEDGMENTS

We thank Anne Horn for her skillful assistance. The Research Council of Norway (Program for Supercomputing) is thanked for a grant of computer time. J.-C.G., L.M., and R.A.M. thank the program “Physique et Chimie du Milieu Interstellaire”, and J.-C.G. thanks “Environnements Planétaires et Origine de la Vie” (INSU-CNRS) and the Centre National d’Etudes Spatiales (CNES) for financial support.

## REFERENCES

- (1) Luna, A.; Mó, O.; Yáñez, M.; Guillemin, J.-C.; Gal, J.-F.; Maria, P.-C. *Int. J. Mass Spectrom.* **2007**, *267*, 125–133.
- (2) Ferris, J. P.; Sanchez, R. A.; Orgel, L. E. *J. Mol. Biol.* **1968**, *33*, 693–704.
- (3) Claisen, L. *Ber. Dtsch. Chem. Ges.* **1903**, *36*, 3664–3673.
- (4) Ben, C. A.; Chucho, J.; Manisse, N.; Pommelet, J. C.; Netsch, K. P.; Lorencak, P.; Wentrup, C. *J. Org. Chem.* **1991**, *56*, 970–975.
- (5) Jachak, M.; Mittelbach, M.; Kriessmann, U.; Junek, H. *Synthesis* **1992**, 275–276.

- (6) Frazza, E. J.; Rapoport, L.  $\beta$ -Cyanovinyl Thio Ethers of Thiazole Compounds, US Patent 3271408, 1966.
- (7) Cole, G. C.; Møllendal, H.; Khater, B.; Guillemin, J.-C. *J. Phys. Chem. A* **2007**, *111*, 1259–1264.
- (8) Guillemin, J.-C.; Breneman, C. M.; Joseph, J. C.; Ferris, J. P. *Chem.—Eur. J.* **1998**, *4*, 1074–1082.
- (9) Xiang, Y.-B.; Drenkard, S.; Baumann, K.; Hickey, D.; Eschenmoser, A. *Helv. Chim. Acta* **1994**, *77*, 2209–2250.
- (10) Askeland, E.; Møllendal, H.; Uggerud, E.; Guillemin, J.-C.; Aviles Moreno, J.-R.; Demaison, J.; Huet, T. R. *J. Phys. Chem. A* **2006**, *110*, 12572–12584.
- (11) Dickens, J. E.; Irvine, W. M.; Nummelin, A.; Møllendal, H.; Saito, S.; Thorwirth, S.; Hjalmarsen, A.; Ohishi, M. *Spectrochim. Acta, Part A* **2001**, *57A*, 643–660.
- (12) The Cologne Database for Molecular Spectroscopy. <http://www.astro.uni-koeln.de/cdms/molecules>.
- (13) Sanchez, R. A.; Ferris, J. P.; Orgel, L. E. *Science* **1966**, *154*, 784–785.
- (14) Bockelée-Morvan, D.; Lis, D. C.; Wink, J. E.; Despois, D.; Crovisier, J.; Bachiller, R.; Benford, D. J.; Biver, N.; Colom, P.; Davies, et al. *Astron. Astrophys.* **2000**, *353*, 1101–1114.
- (15) Coustenis, A.; Schmitt, B.; Khanna, R. K.; Trotta, F. *Planet. Space Sci.* **1999**, *47*, 1305–1329.
- (16) Horn, A.; Møllendal, H.; Guillemin, J.-C. *J. Phys. Chem. A* **2008**, *112*, 11009–11016.
- (17) Kawaguchi, K.; Kasai, Y.; Ishikawa, S.; Ohishi, M.; Kaifu, N.; Amano, T. *Astrophys. J.* **1994**, *420*, L95–97.
- (18) Stoks, P. G.; Schwartz, A. W. *Nature* **1979**, *282*, 709–710.
- (19) Ferris, J. P.; Zamek, O. S.; Altbuch, A. M.; Freiman, H. *J. Mol. Evol.* **1974**, *3*, 301–309.
- (20) Robertson, M. P.; Miller, S. L. *Nature* **1995**, *375*, 772–774.
- (21) Robertson, M. P.; Levy, M.; Miller, S. L. *J. Mol. Evol.* **1996**, *43*, 543–550.
- (22) Nelson, K. E.; Robertson, M. P.; Levy, M.; Miller, S. L. *Origins Life Evol. Biospheres* **2001**, *31*, 221–229.
- (23) Cleaves, H. J., II; Nelson, K. E.; Miller, S. L. *Naturwissenschaften* **2006**, *93*, 228–231.
- (24) Møllendal, H.; Leonov, A.; de Meijere, A. *J. Phys. Chem. A* **2005**, *109*, 6344–6350.
- (25) Møllendal, H.; Cole, G. C.; Guillemin, J.-C. *J. Phys. Chem. A* **2006**, *110*, 921–925.
- (26) Samdal, S.; Møllendal, H.; Hnyk, D.; Holub, J. *J. Phys. Chem. A* **2011**, *115*, 3380–3385.
- (27) Wodarczyk, F. J.; Wilson, E. B., Jr. *J. Mol. Spectrosc.* **1971**, *37*, 445–463.
- (28) Motiyenko, R. A.; Margulès, L.; Alekseev, E. A.; Guillemin, J.-C.; Demaison, J. *J. Mol. Spectrosc.* **2010**, *264*, 94–99.
- (29) Tudorie, M.; Coudert, L. H.; Huet, T. R.; Jegouso, D.; Sedes, G. *J. Chem. Phys.* **2011**, *134*, 074314/1–074314/9.
- (30) Frisch, M. J.; Trucks, G. W.; Schlegel, H. B.; Scuseria, G. E.; Robb, M. A.; Cheeseman, J. R.; Montgomery, J. A., Jr.; Vreven, T.; Kudin, K. N.; Burant, J. C.; Millam, J. M.; Iyengar, S. S.; Tomasi, J.; Barone, V.; Mennucci, B.; Cossi, M.; Scalmani, G.; Rega, N.; Petersson, G. A.; Nakatsuji, H.; Hada, M.; Ehara, M.; Toyota, K.; Fukuda, R.; Hasegawa, J.; Ishida, M.; Nakajima, T.; Honda, Y.; Kitao, O.; Nakai, H.; Klene, M.; Li, X.; Knox, J. E.; Hratchian, H. P.; Cross, J. B.; Bakken, V.; Adamo, C.; Jaramillo, J.; Gomperts, R.; Stratmann, R. E.; Yazyev, O.; Austin, A. J.; Cammi, R.; Pomelli, C.; Ochterski, J. W.; Ayala, P. Y.; Morokuma, K.; Voth, G. A.; Salvador, P.; Dannenberg, J. J.; Zakrzewski, V. G.; Dapprich, S.; Daniels, A. D.; Strain, M. C.; Farkas, O.; Malick, D. K.; Rabuck, A. D.; Raghavachari, K.; Foresman, J. B.; Ortiz, J. V.; Cui, Q.; Baboul, A. G.; Clifford, S.; Cioslowski, J.; Stefanov, B. B.; Liu, G.; Liashenko, A.; Piskorz, P.; Komaromi, I.; Martin, R. L.; Fox, D. J.; Keith, T.; Al-Laham, M. A.; Peng, C. Y.; Nanayakkara, A.; Challacombe, M.; Gill, P. M. W.; Johnson, B.; Chen, W.; Wong, M. W.; Gonzalez, C.; Pople, J. A. *Gaussian 03*, revision B.03; Gaussian, Inc.: Wallingford, CT, 2003.
- (31) Becke, A. D. *Phys. Rev. A* **1988**, *38*, 3098–3100.
- (32) Lee, C.; Yang, W.; Parr, R. G. *Phys. Rev. B* **1988**, *37*, 785–789.
- (33) Møller, C.; Plesset, M. S. *Phys. Rev.* **1934**, *46*, 618–622.
- (34) Purvis, G. D., III; Bartlett, R. J. *J. Chem. Phys.* **1982**, *76*, 1910–1918.
- (35) Scuseria, G. E.; Janssen, C. L.; Schaefer, H. F., III. *J. Chem. Phys.* **1988**, *89*, 7382–7387.
- (36) Peterson, K. A.; Dunning, T. H., Jr. *J. Chem. Phys.* **2002**, *117*, 10548–10560.
- (37) Bailey, W. C. Calculation of Nuclear Quadrupole Coupling Constants in Gaseous State Molecules, 2011. <http://web.mac.com/wcbailey/nqcc>.
- (38) Watson, J. K. G. *Vibrational Spectra and Structure*; Elsevier: Amsterdam, The Netherlands, 1977; Vol. 6, pp 1–89.
- (39) Gordy, W.; Cook, R. L. *Microwave Molecular Spectra*. In *Techniques of Chemistry*; John Wiley & Sons: New York, 1984; Vol. XVII.
- (40) Larsen, N. W.; Schulz, L. *J. Mol. Struct.* **2009**, *920*, 30–39.
- (41) Larsen, N. W.; Steinarsson, T. *J. Mol. Spectrosc.* **1987**, *123*, 405–25.
- (42) Marstokk, K.-M.; Møllendal, H. *J. Mol. Struct.* **1969**, *4*, 470–472.
- (43) Sørensen, G. O. *J. Mol. Spectrosc.* **1967**, *22*, 325–346.
- (44) Ray, B. S. *Z. Phys.* **1932**, *78*, 74–91.
- (45) Motiyenko, R. A.; Margulès, L.; Goubet, M.; Møllendal, H.; Kononov, A.; Guillemin, J.-C. *J. Phys. Chem. A* **2010**, *114*, 2794–2798.
- (46) Kisiel, Z. Programs for Rotational Spectroscopy. <http://info.ifpan.edu.pl/~kisiel/prospe.htm>
- (47) Herschbach, D. R.; Laurie, V. W. *J. Chem. Phys.* **1962**, *37*, 1668–1686.
- (48) Herschbach, D. R.; Laurie, V. W. *J. Chem. Phys.* **1964**, *40*, 3142–3153.
- (49) Esbitt, A. S.; Wilson, E. B. *Rev. Sci. Instrum.* **1963**, *34*, 901–907.
- (50) Townes, C. H.; Schawlow, A. L. *Microwave Spectroscopy*; McGraw-Hill: New York, 1955.